

DexDiffuser: Generating Dexterous Grasps with Diffusion Models

Zehang Weng*, Haofei Lu*,†, Danica Kragic, and Jens Lundell

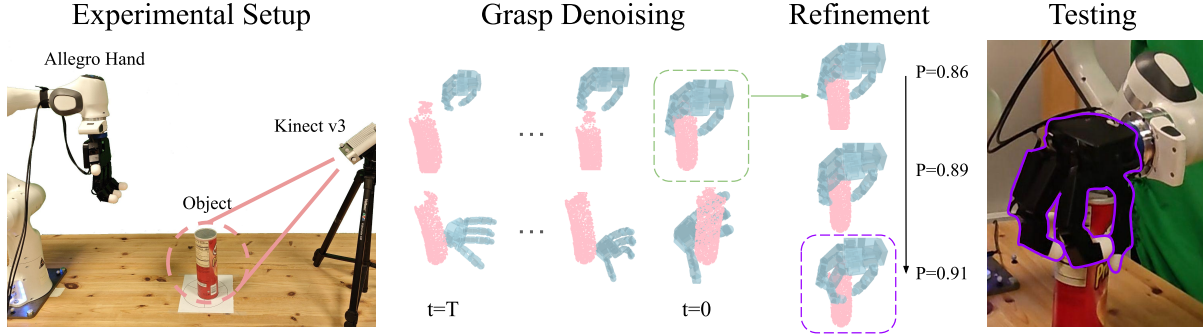


Fig. 1: **DexDiffuser pipeline.** Given a partial point cloud captured by a Kinect v3, DexSampler generated a set of high-quality grasps by gradually removing noise from randomly sampled grasps. Subsequently, the grasps were refined and ranked by the score P from DexEvaluator. The grasp with the highest score was finally selected and executed on the real robot.

Abstract—We introduce **DexDiffuser**, a novel dexterous grasping method that generates, evaluates, and refines grasps on partial object point clouds. **DexDiffuser** includes the conditional diffusion-based grasp sampler **DexSampler** and the dexterous grasp evaluator **DexEvaluator**. **DexSampler** generates high-quality grasps conditioned on object point clouds by iterative denoising of randomly sampled grasps. We also introduce two grasp refinement strategies: **Evaluator-Guided Diffusion** and **Evaluator-based Sampling Refinement**. The experiment results demonstrate that **DexDiffuser** consistently outperforms the state-of-the-art multi-finger grasp generation method **FFHNet** with an, on average, 9.12% and 19.44% higher grasp success rate in simulation and real robot experiments, respectively. Supplementary materials are available at https://yulihn.github.io/DexDiffuser_page/

I. INTRODUCTION

Despite years of research on data-driven grasping [1], generating dexterous grasps for picking unknown objects, similar to the example shown in Fig. 1, remains challenging [2]. One of the main challenges in dexterous grasping is identifying successful grasps within a high-dimensional search space [3].

In this work, we propose the new data-driven dexterous grasping method **DexDiffuser** to address the dimensionality issue. **DexDiffuser** includes **DexSampler**, a new conditional diffusion-based dexterous grasp sampler, and **DexEvaluator**, a new dexterous grasp evaluator. **DexSampler** generates high-quality grasps conditioned on object point clouds by iteratively denoising randomly sampled grasps. In addition to **DexDiffuser**, we also propose two grasp refinement strategies: **Evaluator-Guided Diffusion (EGD)**, which is only applicable for diffusion models, and **Evaluator-based Sampling**

Refinement (ESR), which applies to all dexterous grasp sampling methods.

We experimentally assess **DexDiffuser**'s capability to sample, evaluate, and refine 16-Degrees of Freedom (DoF) Allegro Hand grasps on three visually and geometrically distinctive object datasets in simulation and on one dataset in the real world. **DexDiffuser** is benchmarked against the state-of-the-art multi-finger grasp generation method **FFHNet** [2]. The experimental results indicate that our best method achieves a grasp success rate of 98.77% in simulation and 68.89% in the real world, which is 11.63% and 20.00% higher than the respectively best **FFHNet** model.

Our contribution can be summarized as follows:

- **DexSampler** the novel diffusion-based dexterous grasp sampler (Section IV-B), and **DexEvaluator** the dexterous grasp evaluator (Section IV-C).
- The two refinement strategies **EGD** and **ESR** for improving dexterous grasps (Section IV-D).
- A dataset of 1.7 million successful and unsuccessful Allegro Hand grasp across 5378 objects (Section V).
- A comprehensive experimental evaluation demonstrating the efficacy and real-world applicability of **DexDiffuser** (Section VI).

II. RELATED WORK

This work spans two topics: data-driven dexterous grasping and diffusion models. For brevity, we limit the related works on diffusion models to robotics and, for other areas, refer to the comprehensive survey by Yang et al. [4].

A. Data-Driven Dexterous Grasping

Data-driven dexterous grasp sampling methods primarily fall into three categories: 1) those that generate a contact map on the object's surface [5], [6], [7], 2) those that rely on shape

*Authors with equal contribution. † Corresponding author.

All authors are with the division of Robotics, Perception, and Learning (RPL) at KTH, Stockholm, Sweden. {zehang, haofeil, jelundel, dani}@kth.se

completion [8], [9], [10], [11], [12], [13], [14], [15], or 3) those that train a grasping policy based on Reinforcement Learning (RL) [16], [17] or human demonstrations [18]. The main limitation of the methods in 1) is the assumption of complete object observation, which hinders real-world applications where complete visibility cannot be guaranteed. Methods in 2) are limited because the generated grasp quality is closely intertwined with the completion quality while collecting expensive demonstrations, and the sim-to-real gap limits the methods in 3).

Only a few methods [19], [20], [2] do not adhere to any of the above categories as they generate grasp poses directly on incomplete object observations without shape completion nor training a grasping policy. Our early work [19], focuses on building hierarchical representations of objects on which grasps are sampled. To make learning more tractable, Choi et al. [20] considered one gripper configuration and discretized grasp poses into 6 approach directions and 4 orientations. A discriminative network is trained to score the 24 pre-selected grasp poses for the highest grasp success probability. Qian et al. [2] proposed FFHNet: a Variational Autoencoder (VAE)-based grasp sampler that generates 15-DoF gripper configurations and grasp poses in all of SE(3). Albeit FFHNet reached a 91% grasp success rate in simulation, it was never evaluated on real hardware, leaving the question of real-world performance unanswered. DexDiffuser also produces complete gripper configurations and SE(3) grasp poses but by using diffusion models. Also, we experimentally validate DexDiffuser and FFHNet on real robotic hardware.

B. Diffusion Models in Robotics

Despite being rather recent, diffusion models have already found widespread applicability in motion planning [21], navigation [22], manipulation [23], [24], [25], [26], human-robot interaction [27] and grasping [28]. Of these, the most related to ours is the grasping work by Urain et al. [28], where a diffusion model was trained to generate SE(3) parallel-jaw grasp poses. We propose a diffusion model for generating *dexterous* grasps, meaning that *both* SE(3) grasp poses and high dimensional gripper configurations are generated.

Prior works on diffusion models in robotics have also trained discriminators to evaluate the diffusion-generated samples [24], [25]. In [24], the discriminator scores how realistic point cloud-generated scenes are, while the discriminator in [25] scores how good a generated SE(3) pose is for manipulating an object. Similarly, we use a discriminator to evaluate a generated grasp’s success probability in picking an object.

III. PROBLEM STATEMENT

We consider the problem of sampling and evaluating dexterous grasps \mathbf{G} on partially observed point clouds $\mathbf{O} \in \mathbb{R}^{N \times 3}$, where N is the number of points, for the task of successfully picking up objects. In this work, a grasp $\mathbf{g} \in \mathbf{G} = [\mathbf{p}, \mathbf{r}, \mathbf{q}] \in \mathbb{R}^{9+k}$ is represented by a 3-D position $\mathbf{p} \in \mathbb{R}^3$, a continuous 6-D rotation vector $\mathbf{r} \in \mathbb{R}^6$ [29], and a gripper joint configuration $\mathbf{q} \in \mathbb{R}^k$, where k is the number of

controllable joints. Henceforth, \mathbf{p} and \mathbf{r} are together referred to as the grasp pose and \mathbf{q} as the joint angles. We assume all objects are reachable and singulated, and the object point cloud is segmented from the scene.

We frame the problem of sampling grasps as learning a distribution $P(\mathbf{g} \in \mathbf{G} | \mathbf{O})$ and of evaluating grasps as learning a discriminator $P(S = 1 | \mathbf{g}, \mathbf{O})$, where S is a binary variable representing grasp success ($S=1$) and failure ($S=0$). Henceforth, $P(S = 1 | \mathbf{g} \in \mathbf{G}, \mathbf{O})$ is referred to as the grasp evaluator and $P(\mathbf{g} \in \mathbf{G} | \mathbf{O})$ as the grasp generator. We approximate each of these distributions with a separate Deep Neural Network (DNN) $\mathcal{D}_\theta(\mathbf{g} \in \mathbf{G} | \mathbf{O}) \approx P(\mathbf{g} \in \mathbf{G} | \mathbf{O})$ and $\mathcal{D}_\psi(S = 1 | \mathbf{g} \in \mathbf{G}, \mathbf{O}) \approx P(S = 1 | \mathbf{g} \in \mathbf{G}, \mathbf{O})$, with learnable parameters θ and ψ . The objective then becomes learning θ and ψ from data.

IV. METHOD

We now introduce our framework DexDiffuser to learn the parameters θ and ψ . DexDiffuser consists of two parts: DexSampler and DexEvaluator. We also propose two grasp refinement strategies for improving the grasp success probability.

A. The Basis Point Set Representation

DexDiffuser generates and samples grasps directly on partial object point clouds. In this work, \mathbf{O} is encoded into $\mathbf{f}_\mathbf{O}$ using Basis Point Set (BPS) [30] as this encoding has shown to work well in prior dexterous grasping work [2]. The BPS encoding represents the shortest distance between each point in a fixed set of basis points and all points in \mathbf{O} . The benefit of BPS is that it captures the shape and spatial properties of the object and is of fixed length, which allows for the use of computationally efficient Fully Connected (FC) layers to further process $\mathbf{f}_\mathbf{O}$.

B. Diffusion-based Grasp Sampler

DexSampler is a classifier-free, conditional diffusion model that generates \mathbf{G} conditioned on $\mathbf{f}_\mathbf{O}$. It consists of a forward process that gradually turns data into Gaussian noise and a learnable inverse diffusion process that recovers the data from noise given the condition [31].

In our case, the forward process for incrementally diffusing a successful grasp $\mathbf{g}_0 = [\mathbf{r}_0, \mathbf{p}_0, \mathbf{q}_0]$ over T timesteps is

$$q(\mathbf{g}_{1:T} | \mathbf{g}_0) = \prod_{t=1}^T q(\mathbf{g}_t | \mathbf{g}_{t-1}), \quad (1)$$

$$q(\mathbf{g}_t | \mathbf{g}_{t-1}) = \mathcal{N}(\mathbf{g}_t; \sqrt{1 - \beta_t} \mathbf{g}_{t-1}, \beta_t \mathbf{I}), \quad (2)$$

where β_t is the scheduled noise variance at time step t . To recover the original \mathbf{g}_0 from \mathbf{g}_T , DexSampler learns the reverse diffusion steps by estimating the Gaussian noise added at each t and then removes it as

$$p_\theta(\mathbf{g}_{0:T} | \mathbf{f}_\mathbf{O}) = p(\mathbf{g}_T) \prod_{t=1}^T p_\theta(\mathbf{g}_{t-1} | \mathbf{g}_t, \mathbf{f}_\mathbf{O}), \quad (3)$$

$$p_\theta(\mathbf{g}_{t-1} | \mathbf{g}_t, \mathbf{f}_\mathbf{O}) = \mathcal{N}(\mathbf{g}_{t-1}; \hat{\mu}_\theta(\mathbf{g}_t, t, \mathbf{f}_\mathbf{O}), \hat{\Sigma}_\theta(\mathbf{g}_t, t, \mathbf{f}_\mathbf{O})), \quad (4)$$

where $\hat{\mu}_\theta(\mathbf{g}_t, t, \mathbf{f}_\mathbf{O})$ and $\hat{\Sigma}_\theta(\mathbf{g}_t, t, \mathbf{f}_\mathbf{O})$ is the learnable mean and variance of a Gaussian distribution. The parameters θ are learned by minimizing the loss function

$$L_\epsilon = \|\hat{\epsilon}_t - \epsilon_t\|^2, \quad (5)$$

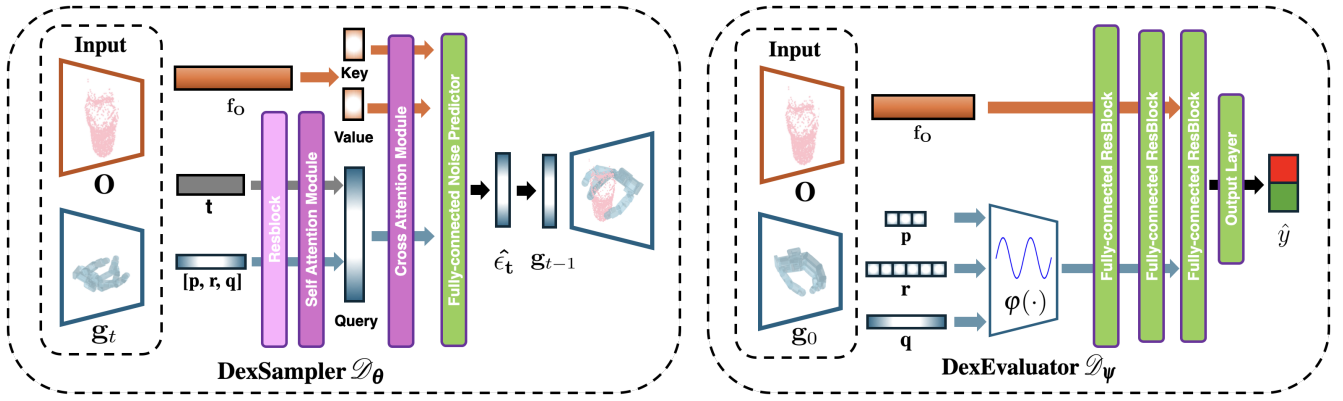


Fig. 2: **Model architecture.** The left image shows the DexSampler. Its input \mathbf{f}_O is processed into a key-value pair while \mathbf{g}_t and t are processed into a query using a self-attention block. The key-value-query triplet is then embedded using a cross-attention block to compute $\hat{\epsilon}_t$. The right image shows the DexEvaluator that predicts grasp success probability given the same \mathbf{f}_O as the DexSampler and \mathbf{g}_0 produced by the DexSampler.

where $\hat{\epsilon}_t \sim \mathcal{N}(\mathbf{g}_{t-1}; \hat{\mu}_\theta(\mathbf{g}_t, t, \mathbf{f}_O), \hat{\Sigma}_\theta(\mathbf{g}_t, t, \mathbf{f}_O))$ and ϵ_t is the ground-truth noise.

The architecture of DexSampler is depicted in Fig. 2, following the practical design of conditional diffusion model [32], [33], [34], [35]. It takes three inputs: \mathbf{f}_O , \mathbf{g}_t , and t and outputs $\hat{\epsilon}_t$ for grasp denoising.

C. Grasp Evaluator

Although DexDiffuser is trained to generate successful grasps, it can still produce unsuccessful ones. Thus, it would be useful if we could only execute grasps with a high probability of succeeding. To this end, we propose DexEvaluator $\mathcal{D}_\psi(S=1|\mathbf{g} \in \mathbf{G}, \mathbf{f}_O)$ to predict the grasp success probability. The architecture of DexEvaluator is shown in Fig. 2 and is inspired by the evaluator in [2]. It takes two inputs: \mathbf{g} and \mathbf{f}_O and outputs S . The main difference to [2] is that we introduce frequency encoding [36] that maps \mathbf{g} into a higher dimensional space before passing it to the evaluator. The map takes the following form

$$\varphi(\mathbf{x}) = [\sin(2^0 \pi \mathbf{x}), \cos(2^0 \pi \mathbf{x}), \dots, \sin(2^{F-1} \pi \mathbf{x}), \cos(2^{F-1} \pi \mathbf{x})], \quad (6)$$

where F specifies the number of sinusoidal functions. $\varphi(\cdot)$ is then separately applied on \mathbf{p} , \mathbf{r} , and \mathbf{q} . Introducing frequency mapping into the evaluator allows it to model better how small changes in \mathbf{g} can lead to large changes in S [37], which requires the model to be sensitive to high-frequency details [36].

The parameters ψ of the DexEvaluator is optimized using the binary cross-entropy loss

$$L(y, \hat{y}) = -y \log(\hat{y}) + (1-y) \log(1-\hat{y}), \quad (7)$$

where y and \hat{y} denote the ground truth and predicted grasp labels, respectively. In Section V, we provide details on the dataset used to train DexEvaluator.

In addition to evaluating grasps, the DexEvaluator can also be used to guide the inverse diffusion process towards more successful grasps or refine already sampled grasps. This we discuss next.

D. Grasp Refinement

The idea behind grasp refinement is to increase the probability of grasp success. In this work, we propose two grasp refinement strategies: EGD, which uses the evaluator to guide the inverse diffusion process, and ESR, which uses the evaluator to refine already sampled grasps.

1) *EGD*: EGD is a form of classifier-guided diffusion. Formally, during the inverse diffusion process, a noisy grasp \mathbf{g}_t is iteratively denoised as

$$p_\theta(\mathbf{g}_{t-1}|\mathbf{g}_t, \mathbf{f}_O) = \mathcal{N}(\mathbf{g}_{t-1}; \mu_\theta(\mathbf{g}_t, t, \mathbf{f}_O) + \lambda \cdot \mathbf{g}_{\text{guide}}, \Sigma_\theta(\mathbf{g}_t, t, \mathbf{f}_O)), \quad (8)$$

$$\mathbf{g}_{\text{guide}} = \nabla_{\mathbf{g}_t} \log \mathcal{D}_\psi(\hat{y}=1|\mathbf{g}_t, \mathbf{f}_O) + \log(T-t+1), \quad (9)$$

where $\mathbf{g}_{\text{guide}}$ is the gradient signal from DexEvaluator modulated by $\log(T-t+1)$. In each step of the inverse diffusion process, $\mathbf{g}_{\text{guide}}$ is used to adjust μ_θ towards more successful grasp. The magnitude of the adjustment is controlled by the parameter λ . The time-dependent modulation term $\log(T-t+1)$ ensures that the guidance is more pronounced in the earlier stages of denoising when the uncertainty in the grasp is higher.

2) *ESR*: Compared to EGD, ESR locally refines already sampled grasps. Prior research on parallel-jaw grasp sampling [37] has demonstrated that many sampled grasps with low evaluator scores often lie spatially close to higher-scoring ones, suggesting that local grasp refinement can improve the grasp success probability. Building upon this insight, we extend the concept of local refinement for parallel-jaw grasps [37], [38] to dexterous grasps, which requires us to refine \mathbf{p} , \mathbf{r} and \mathbf{q} .

Mathematically, local grasp refinement boils down to finding a $\Delta\mathbf{g}$ so that $P(S=1|\mathbf{g}+\Delta\mathbf{g}, \mathbf{f}_O) > P(S=1|\mathbf{g}, \mathbf{f}_O)$. To find $\Delta\mathbf{g}$, we use the Metropolis-Hasting (MH) sampling algorithm as it has been shown to perform well for refining parallel-jaw grasps [38]. To apply MH, we first sample $\Delta\mathbf{g}$ from a known probability distribution and then calculate the acceptance ratio $\alpha = \frac{\mathcal{P}_{\Psi}(S=1|\mathbf{g}+\Delta\mathbf{g}, \mathbf{f}_O)}{\mathcal{P}_{\Psi}(S=1|\mathbf{g}, \mathbf{f}_O)}$. If $\alpha \geq u$, where $u \sim \mathcal{U}[0, 1]$, then $\mathbf{g} = \mathbf{g} + \Delta\mathbf{g}$ otherwise \mathbf{g} is not updated. We refer to this process as ESR-1, as it performs refinement simultaneously for every element of \mathbf{g} .

Because of the higher dimensional search space, local refinement is more challenging for dexterous than parallel-jaw grasps. Therefore, to make the refinement process more tractable, we introduce a two-stage ESR (ESR-2) that first refines \mathbf{p} and \mathbf{r} jointly and only afterward refines \mathbf{q} . The idea behind ESR-2 is first to refine the global grasp parameters \mathbf{p} and \mathbf{r} and only when these are good, refine the local parameters \mathbf{q} .

E. Implementation Details

For training DexSampler, the hyperparameter β_t is controlled using a linear scheduler that moves from 1×10^{-4} to 1×10^{-2} over a total of 100 timesteps. The learning rate is initially set to 1×10^{-4} and controlled by an exponential rate scheduler with $\gamma = 0.9$. DexSampler is trained with a batch size of 16384 for 200 epochs. The learning rate for the DexEvaluator is also set to 1×10^{-4} but controlled with a plateau scheduler. The DexEvaluator is trained with a batch size of 25600 object-grasp pairs for 20 epochs.

For calculating the BPS we randomly sample one set of 4096 basis points. This set is then used to calculate the BPS for every \mathbf{O} in the dataset.

V. DATASET

We used DexGraspNet [39] to generate training grasps and Isaacgym to render 50 \mathbf{O} from different camera views for each object. We collected over 0.7M successful and 0.8M unsuccessful Allegro Hand grasps on 5378 objects of various geometries and scales. Only successful grasps were used to train DexSampler while both successful and unsuccessful grasps were used to train DexEvaluator.

To enhance the dataset with out-of-distribution negative samples, we generated more grasp candidates by jittering the successful grasps in the original dataset. Specifically, a grasp perturbation $\Delta\mathbf{g}_k^{\text{pert}}$ was added for every successful object-grasp pair $(\mathbf{O}_k, \mathbf{g}_k)$. We tested and labeled all the perturbed grasps in Isaacgym and only kept the unsuccessful ones.

The final dataset consisted of 1.7 million grasps, where approximately 40.52% were successful and 59.48% were unsuccessful. We split this dataset into a training set of 4303 objects and a test set of 1,075. We further add 49 objects from the EGAD! dataset [40] and 16 objects from the MultiDex dataset [5] to the test dataset.

VI. EXPERIMENTAL EVALUATION

We experimentally evaluated DexDiffuser in both simulation and the real world, comparing it to the state-of-the-

art grasp sampler and evaluator FFHNet [2]. The specific questions we wanted to address with the experiments were:

- 1) How well can the DexEvaluator predict grasp success?
- 2) What effect does the BPS-encoding have on generating successful grasps?
- 3) To what extent do ESR and EGD improve the grasp quality?
- 4) How well can DexDiffuser generalize to real-world object grasping?

A. Simulation Experiments

All simulation experiments were conducted in Isaac Gym [41] following the setup from [5]. Specifically, test objects were initialized as free-floating objects, and a virtual 16-DoF Allegro Hand was used for grasping each of them. For each of the 1140 test objects, 10 point clouds were rendered from randomly sampled camera poses. Then, all methods generated 20 grasps per point cloud, which amounted to 228,000 test grasps in total. Once an object was grasped, the grasp stability was assessed by applying external forces along the six directions in space for 50 timesteps. A grasp succeeded if the object remained in the hand throughout the stability test.

We also trained a DexSampler with the PointNet++ point cloud encoding [42] to study how different encodings affect grasp performance. We call that network DexDiffuser-PN2 while the BPS network is referred to as DexDiffuser-BPS.

1) *Grasp Evaluation*: To answer the first question, we assessed the DexEvaluator’s grasp prediction accuracy over different numbers of position encodings. The results are presented in Table I. The findings indicate that the DexEvaluator configured with frequencies (10,4,0) achieves the best performance and maintains a balanced accuracy between positive and negative predictions. DexEvaluator with few or no frequencies is biased towards negative predictions, while increasing the number of frequencies from 10 to 20 reduces performance. Thus, we choose the (10,4,0) DexEvaluator in all subsequent experiments.

2) *Grasp Sampling*: To address the second question, we evaluated both FFHNet and DexSampler using either the PointNet++ or BPS encoding. The simulation results are presented in Table II. These results demonstrate that DexSampler, irrespective of the encoding method, consistently outperformed the FFHNet generator across all test

Evaluator	Recall Pos. (%) \uparrow	Recall Neg. (%) \uparrow	Total Acc. (%) \uparrow
No Freq. Enc.	56.47	90.88	73.68
(10,0,0)	77.28	83.42	80.35
(0,10,0)	54.19	91.35	72.77
(0,0,10)	77.13	78.22	77.65
(5,5,5)	55.49	91.78	73.64
(10,10,10)	75.92	78.01	76.97
(10,4,4)	55.32	91.54	73.43
(20,4,0)	74.53	83.68	79.10
(10,4,0)	80.85	80.97	80.91

TABLE I: **Grasp success prediction.** (f_1, f_2, f_3) represent F in (6) for \mathbf{p} , \mathbf{r} , and \mathbf{q} , respectively. \uparrow : The higher, the better.

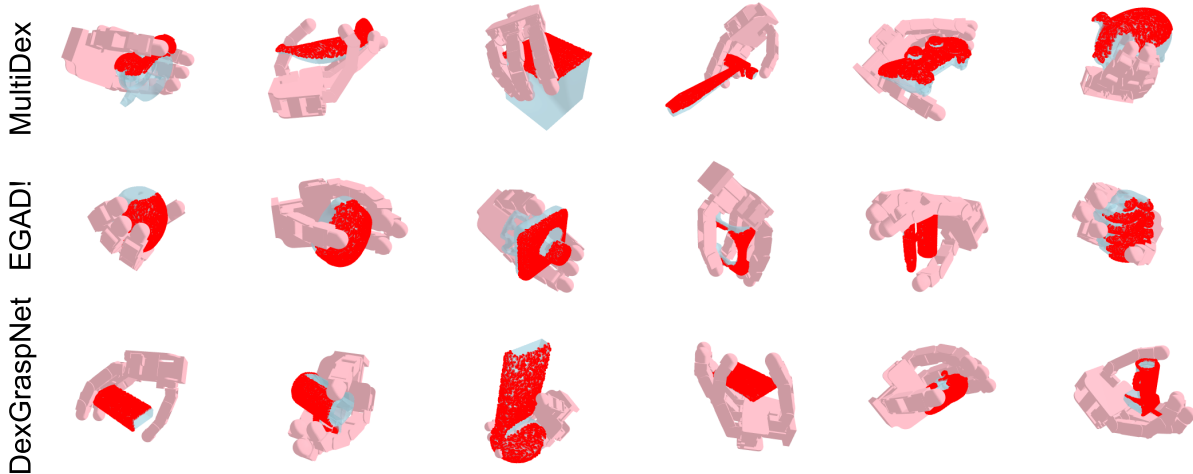


Fig. 3: **Generated grasp examples.** Qualitative evaluation of DexSampler-BPS on objects from different datasets. The grasps, shown in pink, are generated on the partially observed point clouds, shown in red, rendered from the complete meshes, shown in blue.

Method	Dataset		
	MultiDex(%) \uparrow	EGAD! (%) \uparrow	DexGN (%) \uparrow
FFHNet [2]	72.47	87.14	82.16
DexS-PN2	82.28	98.16	81.77
DexS-BPS	87.28	98.62	82.64
FFHNet-ESR-1	71.91	86.77	82.05
FFHNet-ESR-2	72.16	86.86	82.21
DexS-BPS-ESR-1	87.16	98.67	82.57
DexS-BPS-ESR-2	87.47	98.68	82.60
DexS-BPS-EGD	87.63	98.68	82.88
DexS-BPS-EGD-ESR-1	87.41	98.68	82.94
DexS-BPS-EGD-ESR-2	87.78	98.77	82.90

TABLE II: **Grasp success rate of different methods.** The three first rows exclude grasp refinement, while the bottom nine include it. DexS represents the DexSampler. DexGN is short for the DexGraspNet test split. \uparrow : The higher, the better.

datasets. The superior performance underscores the diffusion models’ effectiveness in synthesizing successful grasps. Moreover, DexSampler-BPS performed much better than DexSampler-PN2, indicating that the BPS encoding is less affected by point cloud irregularities, including missing parts and non-uniform density distribution. Finally, Fig. 3 shows some grasps generated by the DexSampler-BPS on the three datasets.

3) *Grasp Refinement*: To answer question 3, we assessed how grasp refinement affected the grasp success rate. The results, presented in Table II, show that ESR improves grasp success rate for both DexDiffuser and FFHNet. For the diffusion-based models, EGD showed marginal improvements, consistent with findings in diffusion-based robot rearrangement scenarios [43]. The two-stage refinement process ESR-2 led to slightly better grasp success rates than ESR-1, giving some evidence to support our hypothesis that it is better to refine global grasp parameters before local ones.

We also evaluated the combination of EGD and ESR

(EGD-ESR) on DexDiffuser by first applying EGD followed by ESR. Although the combination did achieve the highest grasp success rate on the MultiDex and EGAD! datasets, the improvement is, again, marginal compared to the other methods. We hypothesize the reason refinement does not increase the grasp success rates more is because the average grasp classification accuracy, even for the best model, is only 80.91%.

B. Real Robot Experiment

To answer the last question, we evaluated how successful DexDiffuser was at picking objects from real noisy object point clouds using real robotic hardware. The hardware used is shown in Fig. 1 and includes an Allegro Hand attached to the end of a Franka Panda robot and a Kinect V3 placed in a third-person perspective to capture \mathbf{O} . We used a motion capture system to do the extrinsic camera calibration.

We chose 9 different test objects, all shown in Fig. 4, based on their variation in shape and size. Each object was placed in the robot’s workspace in five distinct orientations: 0° , 72° , 144° , 216° , and 288° . All methods generated and ranked 200 grasps per object and orientation. Of these grasps, the best kinematically feasible one was executed on the robot. A grasp was successful if the robot picked the object and kept it grasped while moving to a predefined pose where it rotated the last joint $\pm 90^\circ$.

We evaluated the following methods: FFHNet, FFHNet-ESR-2, DexDiffuser-BPS, DexDiffuser-BPS-ESR-2, DexDiffuser-BPS-EGD and DexDiffuser-BPS-EGD-ESR-2. It is worth highlighting that these methods are only trained on simulated data. The experimental results are summarized in Table III. These results, like the simulation results, show that DexDiffuser consistently outperformed FFHNet across all test objects. The best method for picking real-world objects was DexSampler-BPS-ESR-2, and some of the grasps it produced are shown in Fig. 5. Interestingly,

Real-world experiment Object	# of successful grasps per method and object					
	FFHNet	FFHNet-ESR-2	DexS-BPS	DexS-BPS-ESR-2	DexS-BPS-EGD	DexS-BPS-EGD-ESR-2
1. Crackerbox	2/5	4/5	4/5	5/5	4/5	4/5
2. Sugar box	3/5	4/5	4/5	4/5	4/5	5/5
3. Mustard bottle	3/5	3/5	4/5	5/5	3/5	3/5
4. Bleach cleanser	2/5	2/5	4/5	4/5	5/5	4/5
5. Sprayer	2/5	2/5	3/5	4/5	4/5	4/5
6. Metal mug	2/5	1/5	2/5	3/5	1/5	3/5
7. Goblet	3/5	3/5	5/5	5/5	5/5	4/5
8. Toy plane	0/5	0/5	0/5	0/5	0/5	0/5
9. Pringles	2/5	3/5	2/5	1/5	3/5	2/5
Avg. success rate	42.22%	48.89%	62.22%	68.89%	64.44%	64.44%
Time (ms)	2	490	1692	2188	2548	3036

TABLE III: Experimental results for real-world grasping. DexS represents DexSampler.



Fig. 4: **Experimental objects.** From 1 to 9: cracker box, sugar box, mustard bottle, bleach cleanser, sprayer, metal mug, goblet, toy plane, and pringles

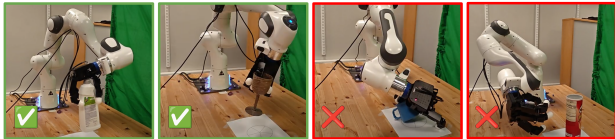


Fig. 5: **Successful and failed grasp examples** from DexSampler-BPS-ESR-2. The first two images successfully grasp the bleach cleanser and the goblet, while the latter two show different failure cases on the metal mug and the pringles.

no methods successfully grasped the toy plane, mainly because the Allegro hand was not strong enough to keep the object secure when the last joint rotated $\pm 90^\circ$, which is demonstrated in the accompanying video¹.

The average grasp success rates in the real world are also consistently lower than in simulation. One rather apparent reason for the decline in performance is that in the real world, grasps are generated on noisy point clouds compared to the clean simulated ones. Another reason is the presence of obstacles that impede the robot’s ability to attain the desired target position. For instance, the first failed grasp in Fig. 5 is because the gripper collided with the table when closing,

while the second failure is because the robot could not reach the intended grasp position due to joint limits. Neither of these failure cases is present in the simulation.

We also report the inference time in Table III. The iterative denoising process makes the diffusion-based methods slower at inference than FFHNet. For instance, the best performing DexDiffuser (DexS-BPS-ESR-2) is 3.5 times slower than the best performing FFHNet (FFHNet-ESR-2).

VII. CONCLUSION

This paper addressed the problem of dexterous grasping under partial point cloud observations. Our proposed solution, DexDiffuser, consists of a conditional diffusion-based grasp sampler and grasp evaluator, BPS-encoded point clouds, and two different grasp refinement strategies. All experiments on the 16-DoF Allegro hand demonstrated that DexDiffuser outperformed FFHNet with an average of 9.12% and 19.44% higher grasp success rate in simulation and real robot experiments, respectively.

The limitations of DexDiffuser are the sim-to-real gap, not accounting for environmental constraints such as collision objects, and the relatively long grasp sampling time. Still, DexDiffuser is one of few data-driven dexterous grasping methods that generate grasps directly on partial point clouds and is evaluated on real hardware. Based on the improvements brought by the diffusion model, we believe such methods can be used to solve other challenging dexterous manipulation tasks, including in-hand manipulation, dexterous grasping in clutter, and joint motion and dexterous grasp planning. Addressing these challenges and the limitations of our method highlights promising future research directions.

REFERENCES

- [1] R. Newbury, M. Gu, L. Chumbley, A. Mousavian, C. Eppner, J. Leitner, J. Bohg, A. Morales, T. Asfour, D. Kragic, D. Fox, and A. Cosgun, “Deep learning approaches to grasp synthesis: A review,” *IEEE Transactions on Robotics*, vol. 39, no. 5, pp. 3994–4015, 2023.
- [2] V. Mayer, Q. Feng, J. Deng, Y. Shi, Z. Chen, and A. Knoll, “Ffhnet: Generating multi-fingered robotic grasps for unknown objects in real-time,” in *2022 International Conference on Robotics and Automation (ICRA)*. IEEE, 2022, pp. 762–769.
- [3] M. T. Ciocarlie, C. Goldfeder, and P. K. Allen, “Dexterous grasping via eigengrasps : A low-dimensional approach to a high-complexity problem,” in *Robotics: Science and Systems Manipulation Workshop - Sensing and Adapting to the Real World*, 2007.

¹https://yulihn.github.io/DexDiffuser_page/

- [4] L. Yang, Z. Zhang, Y. Song, S. Hong, R. Xu, Y. Zhao, W. Zhang, B. Cui, and M.-H. Yang, "Diffusion models: A comprehensive survey of methods and applications," *ACM Computing Surveys*, vol. 56, no. 4, pp. 1–39, 2023.
- [5] P. Li, T. Liu, Y. Li, Y. Geng, Y. Zhu, Y. Yang, and S. Huang, "Gendex-grasp: Generalizable dexterous grasping," in *2023 IEEE International Conference on Robotics and Automation (ICRA)*, 2023, pp. 8068–8074.
- [6] J. Lu, H. Kang, H. Li, B. Liu, Y. Yang, Q. Huang, and G. Hua, "Ugg: Unified generative grasping," 2023.
- [7] A. Wu, M. Guo, and K. Liu, "Learning diverse and physically feasible dexterous grasps with generative model and bilevel optimization," in *Conference on Robot Learning*. PMLR, 2023, pp. 1938–1948.
- [8] S. Ottenhaus, D. Renninghoff, R. Grimm, F. Ferreira, and T. Asfour, "Visuo-haptic grasping of unknown objects based on gaussian process implicit surfaces and deep learning," in *2019 IEEE-RAS 19th International Conference on Humanoid Robots (Humanoids)*. IEEE, 2019, pp. 402–409.
- [9] J. Lundell, E. Corona, T. N. Le, F. Verdoja, P. Weinzaepfel, G. Rogez, F. Moreno-Noguer, and V. Kyrki, "Multi-fingern: Generative coarse-to-fine sampling of multi-finger grasps," in *2021 IEEE International Conference on Robotics and Automation (ICRA)*. IEEE, 2021, pp. 4495–4501.
- [10] J. Lundell, F. Verdoja, and V. Kyrki, "Ddgc: Generative deep dexterous grasping in clutter," *IEEE Robotics and Automation Letters*, vol. 6, no. 4, pp. 6899–6906, 2021.
- [11] M. Van der Merwe, Q. Lu, B. Sundaralingam, M. Matak, and T. Hermans, "Learning continuous 3d reconstructions for geometrically aware grasping," in *2020 IEEE International Conference on Robotics and Automation (ICRA)*, 2020, pp. 11 516–11 522.
- [12] Q. Lu, M. Van der Merwe, and T. Hermans, "Multi-fingered active grasp learning," in *2020 IEEE/RSJ International Conference on Intelligent Robots and Systems (IROS)*, 2020, pp. 8415–8422.
- [13] Q. Lu, M. Van der Merwe, B. Sundaralingam, and T. Hermans, "Multifingered grasp planning via inference in deep neural networks: Outperforming sampling by learning differentiable models," *IEEE Robotics & Automation Magazine*, vol. 27, no. 2, pp. 55–65, 2020.
- [14] M. Liu, Z. Pan, K. Xu, K. Ganguly, and D. Manocha, "Generating grasp poses for a high-dof gripper using neural networks," in *2019 IEEE/RSJ International Conference on Intelligent Robots and Systems (IROS)*, 2019, pp. 1518–1525.
- [15] W. Wei, D. Li, P. Wang, Y. Li, W. Li, Y. Luo, and J. Zhong, "Dvvg: Deep variational grasp generation for dextrous manipulation," *IEEE Robotics and Automation Letters*, vol. 7, no. 2, pp. 1659–1666, 2022.
- [16] Y. Qin, B. Huang, Z.-H. Yin, H. Su, and X. Wang, "Dexpoint: Generalizable point cloud reinforcement learning for sim-to-real dexterous manipulation," in *Conference on Robot Learning*. PMLR, 2023, pp. 594–605.
- [17] P. Mandikal and K. Grauman, "Learning dexterous grasping with object-centric visual affordances," in *2021 IEEE International Conference on Robotics and Automation (ICRA)*, 2021, pp. 6169–6176.
- [18] W. Wan, H. Geng, Y. Liu, Z. Shan, Y. Yang, L. Yi, and H. Wang, "Unidexgrasp++: Improving dexterous grasping policy learning via geometry-aware curriculum and iterative generalist-specialist learning," in *Proceedings of the IEEE/CVF International Conference on Computer Vision*, 2023, pp. 3891–3902.
- [19] M. Popović, G. Kootstra, J. A. Jørgensen, D. Kragic, and N. Krüger, "Grasping unknown objects using an early cognitive vision system for general scene understanding," in *IEEE/RSJ International Conference on Intelligent Robots and Systems*. IEEE, 2011, pp. 987–994.
- [20] C. Choi, W. Schwarting, J. DelPreto, and D. Rus, "Learning object grasping for soft robot hands," *IEEE Robotics and Automation Letters*, vol. 3, no. 3, pp. 2370–2377, 2018.
- [21] J. Carvalho, A. T. Le, M. Baierl, D. Koert, and J. Peters, "Motion planning diffusion: Learning and planning of robot motions with diffusion models," in *2023 IEEE/RSJ International Conference on Intelligent Robots and Systems (IROS)*, 2023, pp. 1916–1923.
- [22] H. Ryu, J. Kim, H. An, J. Chang, J. Seo, T. Kim, Y. Kim, C. Hwang, J. Choi, and R. Horowitz, "Diffusion-edfs: Bi-equivariant denoising generative modeling on se (3) for visual robotic manipulation," in *Proceedings of the IEEE/CVF Conference on Computer Vision and Pattern Recognition*, 2024, pp. 18 007–18 018.
- [23] C. Chi, S. Feng, Y. Du, Z. Xu, E. Cousineau, B. Burchfiel, and S. Song, "Diffusion policy: Visuomotor policy learning via action diffusion," in *Proceedings of Robotics: Science and Systems (RSS)*, 2023.
- [24] W. Liu, Y. Du, T. Hermans, S. Chernova, and C. Paxton, "Strucdiffusion: Language-guided creation of physically-valid structures using unseen objects," in *Proceedings of Robotics: Science and Systems (RSS)*, 2023.
- [25] A. Simeonov, A. Goyal, L. Manuelli, Y.-C. Lin, A. Sarmiento, A. R. Garcia, P. Agrawal, and D. Fox, "Shelving, stacking, hanging: Relational pose diffusion for multi-modal rearrangement," in *Conference on Robot Learning*. PMLR, 2023, pp. 2030–2069.
- [26] L. Chen, S. Bahl, and D. Pathak, "Playfusion: Skill acquisition via diffusion from language-annotated play," in *Conference on Robot Learning*. PMLR, 2023, pp. 2012–2029.
- [27] E. Ng, Z. Liu, and M. Kennedy, "Diffusion co-policy for synergistic human-robot collaborative tasks," *IEEE Robotics and Automation Letters*, 2023.
- [28] J. Urain, N. Funk, J. Peters, and G. Chalvatzaki, "Se(3)-diffusionfields: Learning smooth cost functions for joint grasp and motion optimization through diffusion," in *2023 IEEE International Conference on Robotics and Automation (ICRA)*, 2023, pp. 5923–5930.
- [29] Y. Zhou, C. Barnes, J. Lu, J. Yang, and H. Li, "On the continuity of rotation representations in neural networks," in *Proceedings of the IEEE/CVF Conference on Computer Vision and Pattern Recognition*, 2019, pp. 5745–5753.
- [30] S. Prokudin, C. Lassner, and J. Romero, "Efficient learning on point clouds with basis point sets," in *Proceedings of the IEEE/CVF international conference on computer vision*, 2019, pp. 4332–4341.
- [31] J. Ho and T. Salimans, "Classifier-free diffusion guidance," in *NeurIPS 2021 Workshop on Deep Generative Models and Downstream Applications*, 2021.
- [32] J. Ho, C. Saharia, W. Chan, D. J. Fleet, M. Norouzi, and T. Salimans, "Cascaded diffusion models for high fidelity image generation," *The Journal of Machine Learning Research*, vol. 23, no. 1, pp. 2249–2281, 2022.
- [33] R. Rombach, A. Blattmann, D. Lorenz, P. Esser, and B. Ommer, "High-resolution image synthesis with latent diffusion models," in *Proceedings of the IEEE/CVF conference on computer vision and pattern recognition*, 2022, pp. 10 684–10 695.
- [34] C. Saharia, W. Chan, S. Saxena, L. Li, J. Whang, E. L. Denton, K. Ghasemipour, R. Gontijo Lopes, B. Karagol Ayan, T. Salimans *et al.*, "Photorealistic text-to-image diffusion models with deep language understanding," *Advances in Neural Information Processing Systems*, vol. 35, pp. 36 479–36 494, 2022.
- [35] S. Huang, Z. Wang, P. Li, B. Jia, T. Liu, Y. Zhu, W. Liang, and S.-C. Zhu, "Diffusion-based generation, optimization, and planning in 3d scenes," in *Proceedings of the IEEE/CVF Conference on Computer Vision and Pattern Recognition*, 2023, pp. 16 750–16 761.
- [36] B. Mildenhall, P. P. Srinivasan, M. Tancik, J. T. Barron, R. Ramamoorthi, and R. Ng, "Nerf: Representing scenes as neural radiance fields for view synthesis," in *ECCV*, 2020.
- [37] A. Mousavian, C. Eppner, and D. Fox, "6-dof graspingnet: Variational grasp generation for object manipulation," in *Proceedings of the IEEE/CVF international conference on computer vision*, 2019, pp. 2901–2910.
- [38] A. Murali, A. Mousavian, C. Eppner, C. Paxton, and D. Fox, "6-dof grasping for target-driven object manipulation in clutter," in *2020 IEEE International Conference on Robotics and Automation (ICRA)*, 2020, pp. 6232–6238.
- [39] R. Wang, J. Zhang, J. Chen, Y. Xu, P. Li, T. Liu, and H. Wang, "Dexgraspingnet: A large-scale robotic dexterous grasp dataset for general objects based on simulation," in *2023 IEEE International Conference on Robotics and Automation (ICRA)*, 2023, pp. 11 359–11 366.
- [40] D. Morrison, P. Corke, and J. Leitner, "Egad! an evolved grasping analysis dataset for diversity and reproducibility in robotic manipulation," *IEEE Robotics and Automation Letters*, vol. 5, no. 3, pp. 4368–4375, 2020.
- [41] V. Makoviychuk, L. Wawrzyniak, Y. Guo, M. Lu, K. Storey, M. Macklin, D. Hoeller, N. Rudin, A. Allshire, A. Handa *et al.*, "Isaac gym: High performance gpu based physics simulation for robot learning," in *Thirty-fifth Conference on Neural Information Processing Systems Datasets and Benchmarks Track (Round 2)*, 2021.
- [42] C. R. Qi, L. Yi, H. Su, and L. J. Guibas, "Pointnet++: Deep hierarchical feature learning on point sets in a metric space," *Advances in neural information processing systems*, vol. 30, 2017.
- [43] W. Liu, Y. Du, T. Hermans, S. Chernova, and C. Paxton, "Strucdiffusion: Language-guided creation of physically-valid structures using unseen objects," in *RSS*, vol. 1, 2023, p. 3.